Tough, self-healing hydrogels capable of ultrafast shape changing

Zhen Jiang, Broden Diggle, India C.G. Shackleford and Luke A. Connal[a]*

Dr. Z. Jiang, Mr. B. Diggle, Ms. I. Shackleford and Associate Prof. Luke A. Connal
Research School of Chemistry
Australian National University
Canberra ACT 2601, Australia
E-mail: luke.connal@anu.edu.au

Keywords: Shape changing hydrogels, self-healing, multi-functional hydrogel, multiple dynamic bonds, mechanically strong

Abstract. Achieving multifunctional shape changing hydrogels with synergistic and engineered material properties is highly desirable for their expanding applications, yet remains an ongoing challenge. The synergistic design of multiple dynamic chemistries enables new directions for development of such materials. Herein, we propose a molecular design strategy based on hydrogel combining acid-ether hydrogen bonding and imine bonds. Our approach utilizes simple and scalable chemistries to produce a doubly dynamic hydrogel network, which features high water uptake, high strength and toughness, excellent fatigue-resistance, fast and efficient self-healing, as well as super-fast, programmable shape changing. Furthermore, deformed shapes could be memorized due to a large thermal hysteresis. This new type of shape changing hydrogel is expected to be a key component in future biomedical, tissue and soft robotic device applications.

Introduction

Nature's blueprints for shape changing materials may be found everywhere, for example the Venus flytrap,[1] pine cones,[2] jellyfish[3] and sea cucumbers[4]. Inspired by these, chemists have developed a variety of synthetic shape changing materials including shape memory polymers,[5] liquid crystalline polymers,[6] hydrogels,[7] and carbon-based nanomaterials.[8] Among these, hydrogels are particularly attractive due to their high water uptake, an ability to significantly change their volume in response to stimuli,[7c] programmable shape

changeability,[9] and similar physiochemical properties to biological soft tissues. These properties enable them to be extensively applied in many fields such as soft robotics,[10] microfluidics,[11] three-dimensional (3D) cell cultures,[12] surgery,[13] and biomedical engineering.[14]

The actuation mechanism of a hydrogel is through changes of the water uptake in the network, which may be triggered by a shift in the hydrophilicity-hydrophobicity balance upon external stimuli.[9] Most recently, great progress has been made in achieving complex 3D deformations[15] and fast responsiveness.[16] However, a single shape changing function often does not meet all of the requirements for practical applications. Therefore, development of shape changing hydrogels combining multiple functions is highly desirable. For example, high strength and toughness[17] has been achieved in order to withstand daily mechanical stress. Self-healing properties[7f, 18] enhance the reliability and extend the lifetime of shape changing materials. Other properties including shape memory,[19] 3D printability,[15d, 17a] colour changing,[20] and biocompatibility[14] have also been incorporated. Yet these reported shape changing hydrogels usually possess only one of these added functionalities. To the best of our knowledge, there has been a lack of simple and efficient strategies to integrate diverse functions into a single hydrogel system while achieving fast response and programmable shape changing simultaneously.

Introducing dynamic bonds into polymers represents an attractive approach for imparting multiple material properties in a synergistic way.[21] Due to their reversible nature, under equilibrium conditions, many material properties such as high mechanical strength,[22] viscoelasticity,[23] self-healing[24], shape memory[5a, 25] and 3D printability[26] may be readily tunable. Additionally, dynamic bonds show high responsivity to stimuli, enabling materials to have environmental adaptation and self-repair.[27] Integrating multiple orthogonal dynamic

chemistries could enable unique properties and functions[21d] that are not easily achievable through single dynamic bonds such as multi-shape memory,[28] fast self-healing,[29] and combinations of high strength, toughness, fast shape recovery, and fatigue resistance.[22d, 30] Moreover, Draper *et al.* fabricated a double network consisting of pH and photoresponsive dynamic bonds, which enabled a high degree of spatial control over the gel's rheological and mechanical properties.[31] Rational design of these multi-dynamic networks is a key strategy toward polymers that possesses multiple targeted properties without mutual interference. To demonstrate this concept, hydrogen bonding between methacrylic acid (MAA) and oligo(ethylene glycol) methacrylate (OEGMA) was utilized as the first network; providing function that effectively dissipates energy under mechanical deformation, facilitates self-healing, and causes the innate hydrophilicity of the hydrogel. Furthermore, owing to its COOH groups, the copolymer poly(MAA-*co*-OEGMA) may act as a functional polymer platform for facile attachment of benzaldehyde units, further incorporating a dynamic covalent imine bond as a second network. The presence of a small fraction (0.01 mol% to 2.10 mol%) of imine bonds serves as permanent crosslink to protect the integrity of network, further stabilizing the physically crosslinked hydrogel, and contributing to self-healing. After a freeze-thaw process, the resultant doubly dynamic hydrogel still contains quite a high water uptake , while combining high strength and toughness, fast and efficient self-healing, excellent fatigue-resistance, super-fast actuation, programmable 3D deformations, and memory function. The advantages of using such a multi-functional hydrogel is further demonstrated through an ability to lift heavy objects in a reversible and repeatable way upon thermal stimulus. To the best of our knowledge, no other shape changing hydrogels with all these features have been reported.

Results and Discussion

Materials Design and Preparation. It is well known that the Bronsted acid PMAA could form hydrogen bonds with oxygen atoms of the Lewis basic OEGMA chains.[32] This complexation is highly dynamic (relaxation time ≈ 0.1 s) [33] and is stabilized by hydrophobic interactions. Moreover, we have found that OEGMA provides quite strong solvation effects due to the relatively long oligo(ethylene glycol) side chain.[34] [35] Inspired by these results, we selected this acid-ether hydrogen bonding model for our design. First, we synthesized the copolymer of PMAA and OEGMA using Reversible Addition-Fragmentation chain Transfer (RAFT) polymerization. The final random copolymer poly(MAA-*co*-OEGMA) contains ~75 mol % MAA, as determined from ^{1}H-NMR (Figure S1A). The theoretical molecular weight was calculated to be 35,500 g mol^{-1} using monomer conversion.[36] FTIR analysis shows an absence of C=O stretching at 1750 cm^{-1} indicating a lack of monomeric carboxylic acids and that all of the MAA has been associated (Figure S2A).[37] The appearance of a peak at 1700 cm^{-1} suggests the formation of hydrogen bonds between two carboxylic acids in PMAA (Figure S2A). The observed peak at 1730 cm^{-1} could be assigned to the ester carbonyl group in OEGMA and the hydrogen bonded associations between MAA and OEGMA.[37] The stronger signal intensity observed at 1730 cm^{-1} compared to that at 1700 cm^{-1} may suggest that most of the MAA units have formed acid-ether hydrogen bonds with OEGMA. The poly(MAA-*co*-OEGMA) has a diffusion coefficient of $4.4 \pm 0.03 \times 10^{-11}$ m^2 s^{-1} in water determined by diffusion-ordered spectroscopy (Figure S3), and thus has a hydrodynamic diameter of approximately 12 ± 0.2 nm suggesting the formation of aggregates.[34a] This result indicates that hydrogen bonding is strong and stable in water [32a, 38].

Along with forming strong inter and intra-molecular hydrogen bonding,[29] carboxylic acid groups in the copolymer allow for facile attachment of benzaldehyde units to the polymer via a simple esterification with commercially available 4-hydroxybenzaldehyde. The 4-

hydroxybenzaldahyde serves two functions: one is to form an aldehyde group for subsequent formation of dynamic imine bonds, the other is to provide hydrophobicity to further stabilize the hydrogen bonding.[38] As shown in Figure S2B, a peak at 1730 cm^{-1} was observed and assigned to an aldehyde group, indicating successful modification. NMR studies confirmed 25% conversion of carboxylic acid groups to benzaldehydes (Figure S1B), yielding a copolymer with a final composition of poly(MAA_{116}-*co*-BA_{39}-*co*-$OEGMA_{45}$). Furthermore, DOSY NMR in $CDCl_3$ revealed the same diffusion coefficient of $2.4 \pm 0.8 \times 10^{-11}$ m^2 s^{-1} for the aldehyde groups as other groups in the polymer chain (Figure S4), indicating that the aldehyde group is covalently linked to the polymer.

The copolymer, poly(MAA_{116}-*co*-BA_{39}-*co*-$OEGMA_{45}$), was then crosslinked with ethylenediamine (EDA) with a molar ratio of 1:0.25 (aldehyde: EDA) to form imine bonds. The dynamic imine bond were selected owing to their dynamic covalent nature and fast reaction kinetics[21a, 39]; we previously demonstrated that a very small amount of imine crosslinker (0.08 mol%) could enable very fast self-healing (within 30 mins)[39a]. EDA was chosen as a simple and readily available diamine. The crosslinked hydrogel was further purified by dialysis against DI water and ethanol. FTIR spectra of the EDA crosslinked polymer (Figure S5) confirms the presence of an imine bond, with a characteristic imine peak at 1625 cm^{-1}, indicating successful formation of dynamic imine bonds. It is worth to noting that the characteristic peak of 4-hydroxybenzaldehyde (carbonyl band at 1664 cm^{-1} ascribed to aldehyde group) could not be found in the EDA crosslinked polymer (Figure S5B), indicating high purity of the hydrogel.

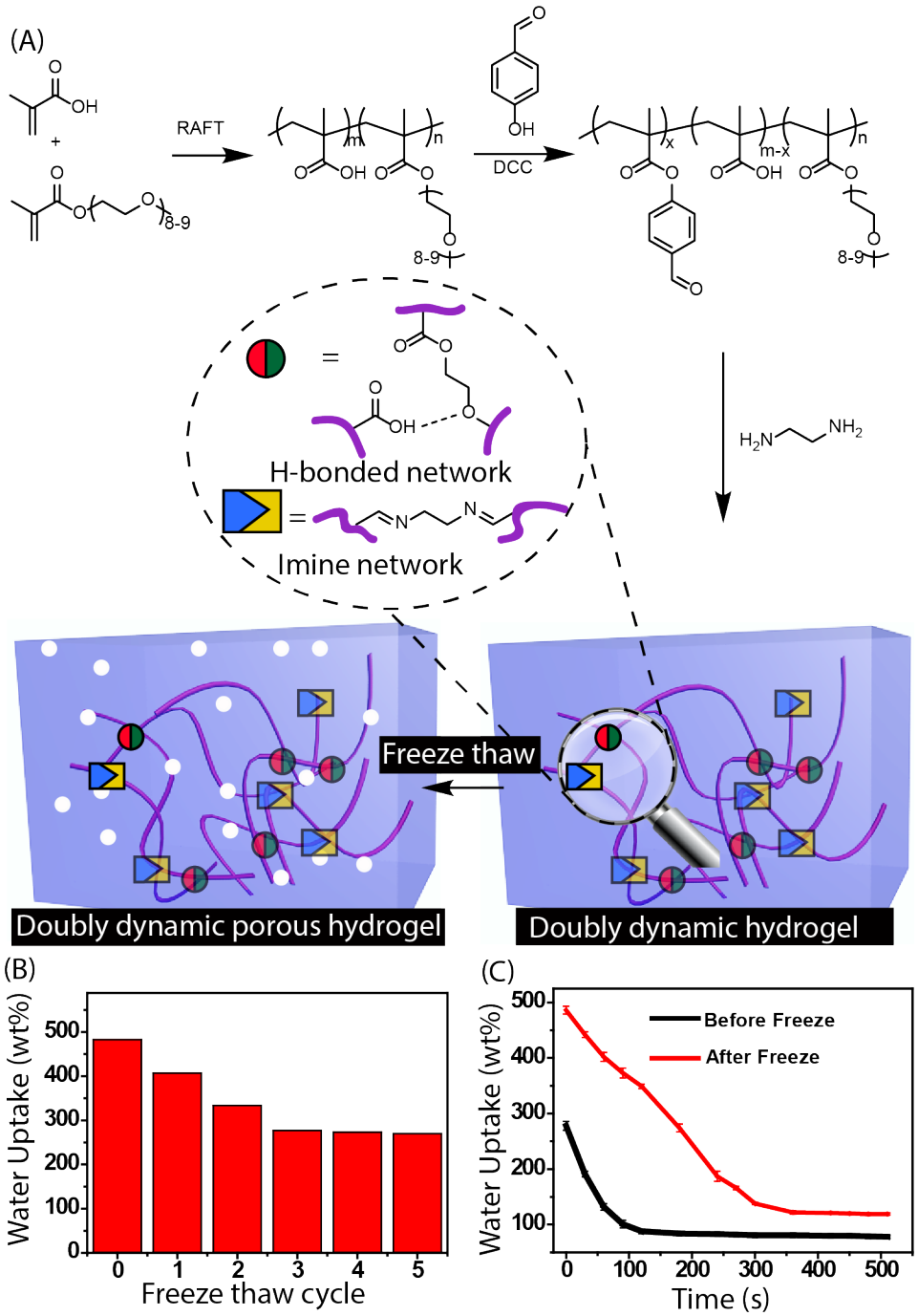

Figure 1. Fabrication of a doubly dynamic freeze-thawed hydrogel and its characterization. (A) Schematic representation of the molecular design and preparation of the doubly dynamic network. (B) Water uptake of the freeze-thawed hydrogel as a function of different cycles. (C) Deswelling behaviour of the EDA crosslinked hydrogel and freeze-thawed hydrogel over time at 50°C water bath.

In order to further enhance hydrogen bonding and to increase transport of water molecules in the hydrogel network, the gel was subjected to freeze/thaw cycling.[17b, 40] The FTIR spectra (Figure S5) of the freeze/thawed hydrogel was measured. A significant broadening and an increase in signal intensity of hydroxyl groups (3100-3600 cm^{-1}) was observed (Figure S5A). Both the intensity of the peak at 1700 cm^{-1} as well as the peak at 1730 cm^{-1} were found to have increased after the freeze-thaw process (Figure S5). These results demonstrate that both the intramolecular hydrogen bonds within carboxylic acids, and the intermolecular hydrogen bond with OEGMA could be strengthened after the freeze-thaw process. Additionally, water uptake of the freeze/thawed hydrogels was studied. With an increasing number of freeze-thaw cycles, a decrease in the amount of water uptake was observed initially however this plateaued after the third freeze-thaw cycle (Figure 1B). Notably, the water uptake of the freeze-thawed sample (Figure 1B, Figure S6) after repeated cycles was still very high (278 ± 6 wt%), despite significantly enhanced hydrogen bonding, which is distinct from the low water uptake (≈ 0-60 wt%) often found in hydrogen bonded hydrogels after freeze-thawing.[41]

Furthermore, we explored whether water diffusion through the hydrogel, which significantly affects the shape changing speed,[16a, 17c, 42] could be improved after freeze-thawing. Both hydrogels (before and after freeze-thaw) were immersed into a 50°C water bath, which is above the lower critical solution temperature (LCST) of uncrosslinked poly(MAA_{116}-*co*-BA_{39}-$OEGMA_{45}$) in water (Figure S7), and the deswelling behaviour of both hydrogels were recorded as function of time. Both swollen hydrogels tended to dehydrate and significantly lose water after immersion in water at higher temperatures, due to the disruption of the hydrophilic/ hydrophobic balance (Figure 1C). Importantly, it can be seen that the equilibrium time for shrinking from a fully swollen state to a fully collapsed state for a freeze-thawed sample (3cm*2cm*1mm) is only 2 min, which is much faster than that of the original EDA crosslinked hydrogel with the same dimensions which requires around 7 min to achieve a

thermal-induced equilibrium state. The faster water diffusion observed in freeze-thawed hydrogels could be attributed to the formation of microporous structures after freeze-thawing (Figure S8). Indeed, similar observations have been reported in freeze-thawed poly(N-isopropylacrylamide) (PNIPAM) hydrogels.[17b] Dynamic Mechanical Analysis (DMA) results showed an increased glass transition temperature of the freeze-thawed hydrogel compared to the original sample (Figure S9). It can be seen that the tan δ peak, representative of the glass transition region, for the freeze-thawed hydrogel is much broader than that of its non-freeze-thawed counterpart, which may be due to decreased chain mobility and an increase in the heterogeneity of the system.[43] In addition, freeze-thawing led to an enhancement of the dynamic mechanical properties, e.g., the freeze-thawed sample showed G' ≈ 2.7 MPa, which is 4 times as large as that of the sample before freeze thawing (G' ≈0.6 MPa) at 25 °C. These results indicate that both the mechanical properties and water diffusion speed could be improved simultaneously through the freeze-thaw process.

Mechanical and self-healing properties. A critical design criteria for our approach was the ability of the dynamically crosslinked hydrogel to dissipate energy when stretched. We achieved this through a double network consisting of dynamic noncovalent hydrogen bonding and dynamic covalent imine bonds. This property could be achieved due to acid-ether hydrogen bonding behaving as sacrificial bonds,[44] to effectively dissipate energy when stretched,[45] while the small amount of dynamic imine crosslinks can protect the integrity of the hydrogel after the weak network was fractured. A 5×1×0.6 cm rectangular sample of the freeze-thawed hydrogel was capable of holding a load of 1 kg without breaking (Figure 2A). Additionally, the elasticity of the freeze-thawed hydrogel was demonstrated through its prompt recovery to its original size after removal of an applied force (Figure 2A, Movie 1). Before measuring the mechanical properties of the freeze-thawed hydrogels, tensile properties

of hydrogen bond crosslinked poly(MAA-*co*-OEGMA) were measured. Intriguingly, it showed exceptional stretchability (Figure S11A, Figure S11B). Even after stretching over 7000% of its original size it was not possible to fracture this sample. In fact, full limits could not be recorded due to size restrictions of the instrument. Such high stretchability may be due to the highly reversible nature of acid-ether hydrogen bonds which may form new bonds when the material undergoes network sliding after it is fractured by a mechanical force.[46] Furthermore, the sample was still not fractured after post-modification with 4-hydroxybenzaldehyde although it was measured to have slightly higher tensile strength due to the hydrophobic interactions (Figure S12). However, after crosslinking with EDA (a molar ratio of aldehyde: EDA 1 : 0.25), the break strain was substantially reduced to 773 ± 5.1% while the breaking strength increased to 1.6 ± 0.2% MPa. Further freeze-thaw treatment resulted in an increased breaking strength of 3.0 ± 0.3% MPa but a lower breaking strain (520 ± 4.5%), which could be explained as a result of increased rigidity of the network after freeze-thawing.[40b]

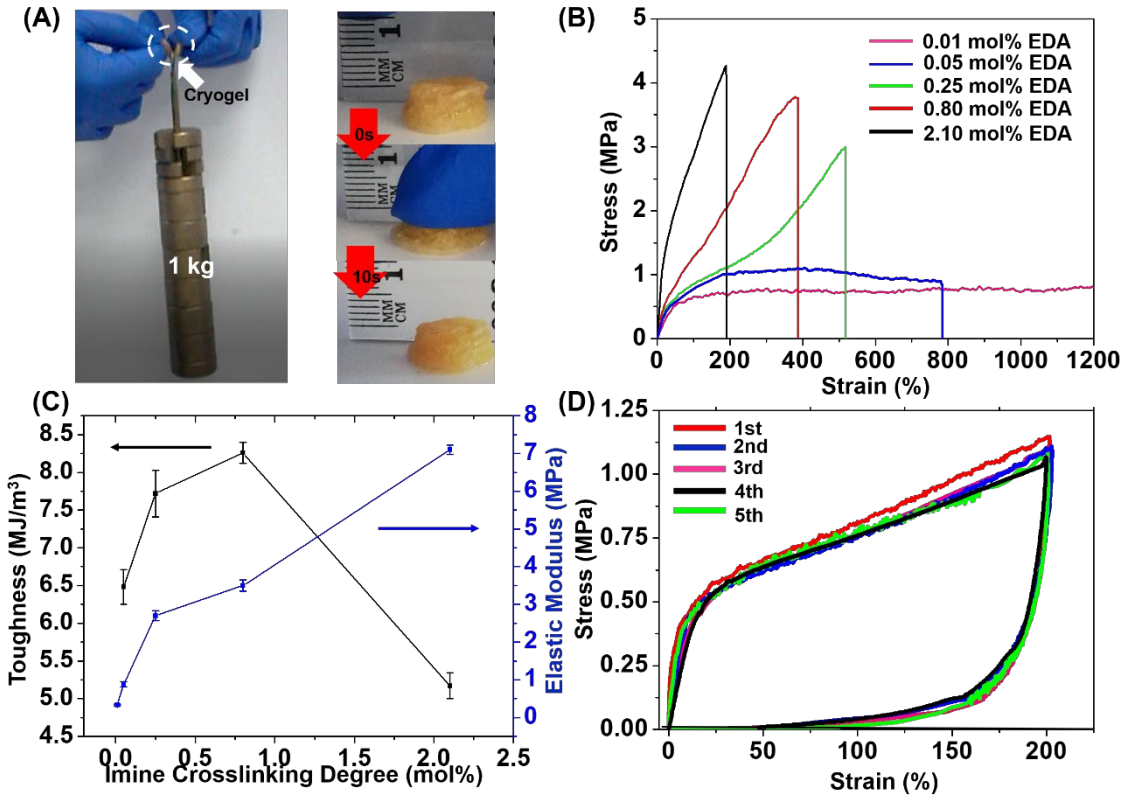

Figure 2. Mechanical properties of freeze-thawed hydrogels. (A): Photographs showing the (left) strength of the gel slab which is capable of lifting 1kg weight and (right) fast recovery which could resist the compression by hand and recovered immediately after removal of the force. (B) Stress–strain curves, showing significant changes in strength with small amount of dynamic imine crosslinking is introduced (C) Toughness and elastic modulus of the freeze-thawed hydrogels with different dynamic imine crosslinking density. (D) Five successive cyclic tensile loading−unloading curves of freeze-thawed hydrogel with EDA crosslinking density of 0.25 mol% at a strain of 200% with 5 min resting between tests.

The crosslinking density of the dynamic imine bond could significantly affect the material properties. We investigated this systematically by adjusting the amount of the EDA crosslinker. Figure 2B shows the tensile stress-strain curves of the synthesized hydrogels with varied imine crosslinking densities. When the content of EDA was increased from 0.01 mol% to 2.10 mol%, a significant increase of tensile strength and Young's modulus, and a decrease

in breaking strain were observed. Meanwhile, the toughness of the hydrogels increased with increasing crosslinking density from 0.01-0.80 mol%, while it decreased at much higher crosslinking density due to much shorter chains between crosslinker sites (Figure 2C). It was found that all of the doubly dynamic freeze-thawed hydrogels demonstrated superior mechanical properties, including tensile strength (650 kPa-4.3 MPa), breaking strain (198->7000%), Young's modulus (0.42-7.2 MPa) and toughness (6.4-8.3 MJ/m^3). These results indicate that the mechanical properties of this freeze-thawed hydrogel are tunable over a wide range. The excellent mechanical properties of these freeze-thawed hydrogels are comparable or even superior to existing shape changing hydrogels (breaking strength ≈30kpa-2MPa, breaking strain ≈ 10%-1000%).[7e, 17c, 17d, 18b, 35, 47] The temperature responsive swelling was also effected by crosslink density (Figure S10). The freeze-thawed hydrogel with higher EDA content showed less obvious shape change, presumably due to higher imine crosslink density. Considering its excellent breaking strain and tensile strength, along with significant swelling above the phase transition temperature, the freeze-thawed hydrogel sample with an EDA content of 0.25 mol% was selected as the ideal candidate for further investigation.

Fatigue resistance is needed to sustain cyclic actuations in practical applications.[48] Therefore, we measured the fatigue resistance of the freeze-thawed hydrogel through consecutive loading-unloading cycle tests at a maximum strain of 200% with 5 min of resting between two tests. Apparent hysteresis loops were observed on loading–unloading curves, indicating the freeze-thawed hydrogel could dissipate energy effectively through the rupture of dynamic hydrogen bonding; as much as 1.67 ± 0.28 MJ m^{-3} (Figure 2D). Only 12% of the dissipated energy observed in cycle 1 was lost in cycle 2, indicating quick and efficient recovery of the hydrogel (Figure S12). However, full recovery of the dissipated energy was not observed due to permanent breakage of a small amount of covalent bonds during loading. The areas of the hysteresis loops remain almost constant over consecutive cycle tests suggesting great fatigue

resistance (Figure S12). This could be due to fast reorganization of the reformed hydrogen bonds under deformation combined with the presence of dynamic covalent bonds which may provide the necessary elasticity.[49]

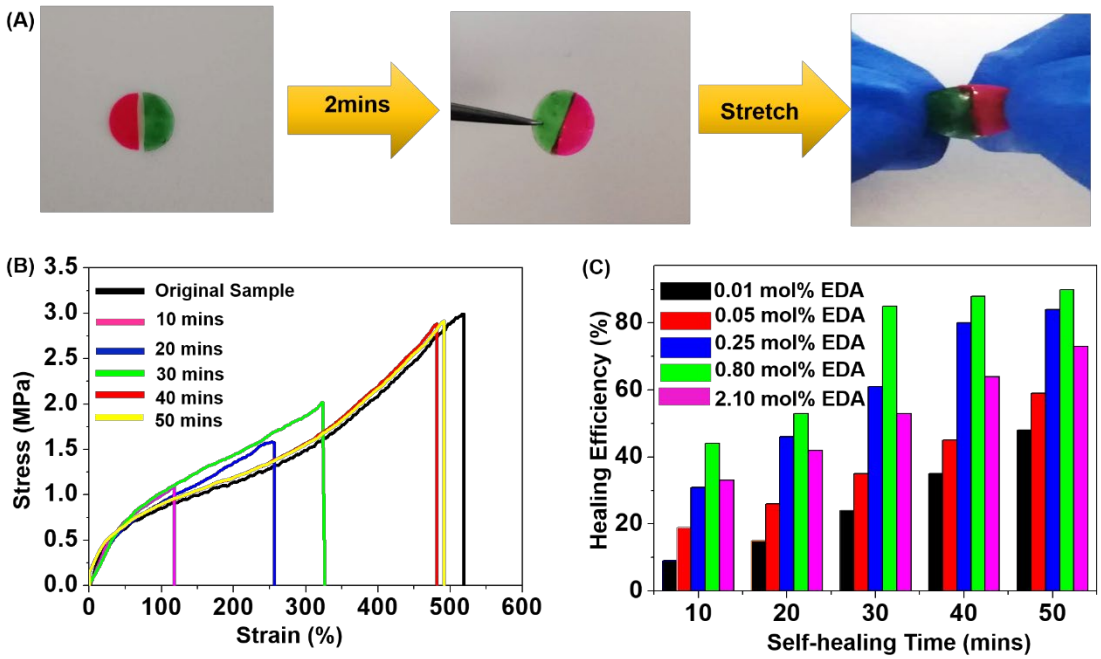

Figure 3. Self-healing properties of freeze-thawed hydrogels. (A) Photographs of a disk-shape freeze-thawed hydrogel of different colours cut into two pieces (left) and rejoined back into disk after healing at 2 mins (middle) and (right) then further undergoes a slight stretch. (B) Stress–strain curves for original and healed freeze-thawed hydrogel samples containing 0.25 mol% EDA after different healing times. (C) Dependence of the healing efficiency of the freeze-thawed hydrogels with different crosslinking densities on time.

It is widely acknowledged that achieving both excellent mechanical properties and efficient self-healing is a significant challenge.[22d, 50] This is because noncovalent bonds, which result in good self-healing properties, are intrinsically weak, while relatively strong covalent dynamic bonds restrict the motion of chains and reduce self-healing efficiency. In this study, however, engineering hydrogels with loosely crosslinked dynamic covalent imine bonds as well as tightly crosslinked hydrogen bonding is expected to solve this dilemma.[39a] In order to

study the hydrogel's self-healing ability, two disk-shaped dry freeze-thawed hydrogels with different colors were cut through their center into two pieces which were subsequently kept in close contact with a tweezer at room temperature (Figure 3A). After only 2 minutes, the two cut pieces were tightly merged into one single piece such that the recovered sample could withstand stretching deformation without breakage. To quantitatively investigate self-healing efficiency, stress-strain properties between the original and healed samples at varied healing times were studied (Figure 3B). It demonstrated that both the breaking stress and strain quickly increased with healing time. Notably, the freeze-thawed hydrogel manifested rapid and efficient self-healing behaviour at room temperature without any external stimulus: an 84% recovery of the original fracture stress (tensile strength) was observed after only 40 mins of self-healing. This fast and efficient self-healing performance can be due to fast exchange kinetics of both imine and hydrogen bonding on the crack's surface. Furthermore, the glass transition temperature of the freeze-thawed hydrogel (Figure S10) was measured to be around 28°C which is very close to ambient temperature, indicating sufficient chain mobility to facilitate self-healing.[51] Furthermore, the self-healing efficiency of freeze-thawed hydrogels were studied as a function of healing time with imine crosslinking densities. It was observed that healing efficiency was improved with increasing crosslinking density from 0.01 mol% to 0.80mol% (Figure 3C) – the sample containing 0.25 mol% EDA reached a higher level of self-healing efficiency up to 79 ± 2% at 25 °C after only 40min. On the other hand, the sample with highest imine crosslinking density (2.1 mol%) exhibited compromised self-healing efficiency (only up to 63 ± 3% for 40 mins), which may be ascribed to reduced chain mobility.[52]

Shape Transformation: Another significant challenge for hydrogel actuators is attaining fast and programmable shape changes. One method to create polymer actuators is through using bilayer systems, where one layer is non-responsive and the other is stimuli responsive.[7f] The

beauty of our procedure was that we could easily integrate this design into our system. We prepared a non-responsive polymer layer by using the aforementioned sample components but changing the composition to have significantly more PMAA (85 mol% in feed ratio). The polymer's final composition was poly(MAA$_{136}$-*co*-BA$_{34}$-OEGMA$_{30}$). At this composition, the copolymer could not be dissolved in water at any temperature and the LCST could not be observed due to formation of stronger hydrophobic intra-molecular acid–ether hydrogen bonding.[32a, 38] This observation is consistent with previous work wherein the cloud point of poly(MAA-*co*-OEGMA) could not be observed when the OEGMA content was decreased beyond a certain threshold.[32a] As such, a nonresponsive layer was fabricated with this copolymer using the same procedures described in the experimental section. The bilayer was prepared by assembling a freeze-thawed hydrogel film (1.5×0.5×0.2 cm) with a non-responsive gel as the bottom layer (Figure 4A). Our versatile materials enabled fabrication of thin films with thickness of hundreds of micro-meters without breakage, which is desirable for achieving fast actuation.[42] Also, the self-healing ability provided a strong interaction between the interfaces due to the exchange of dynamic bonds, overcoming the limitations of delamination in traditional bilayer hydrogels.[53] Thermally induced shape changing of such bilayer freeze-thawed hydrogels was examined by immersing the equilibrium swollen samples in water at 50 °C. The bilayer freeze-thawed hydrogel generated a superfast bending movement and formed a roll with a bending angle of 384° in just 8 s (Figure 4B, Movie 2), the roll then recovered to its original shape in 40 s after it was returned to room temperature. In contrast, the non-freeze-thawed sample showed a much slower bending speed, taking 1 min to achieve its maximum bending angle (Figure S13). The superfast shape changing speed of the freeze-thawed hydrogels could be ascribed to the formation of micro-porosity structures induced by ice crystals during the freeze-thaw process (Figure S8).[17b] Importantly, the shape changing speed of this hydrogel is comparable or superior to previously reported rapid response hydrogels (Response time ≈ 10s-20min).[7d, 7e, 16b, 17a, 17c, 42, 54]

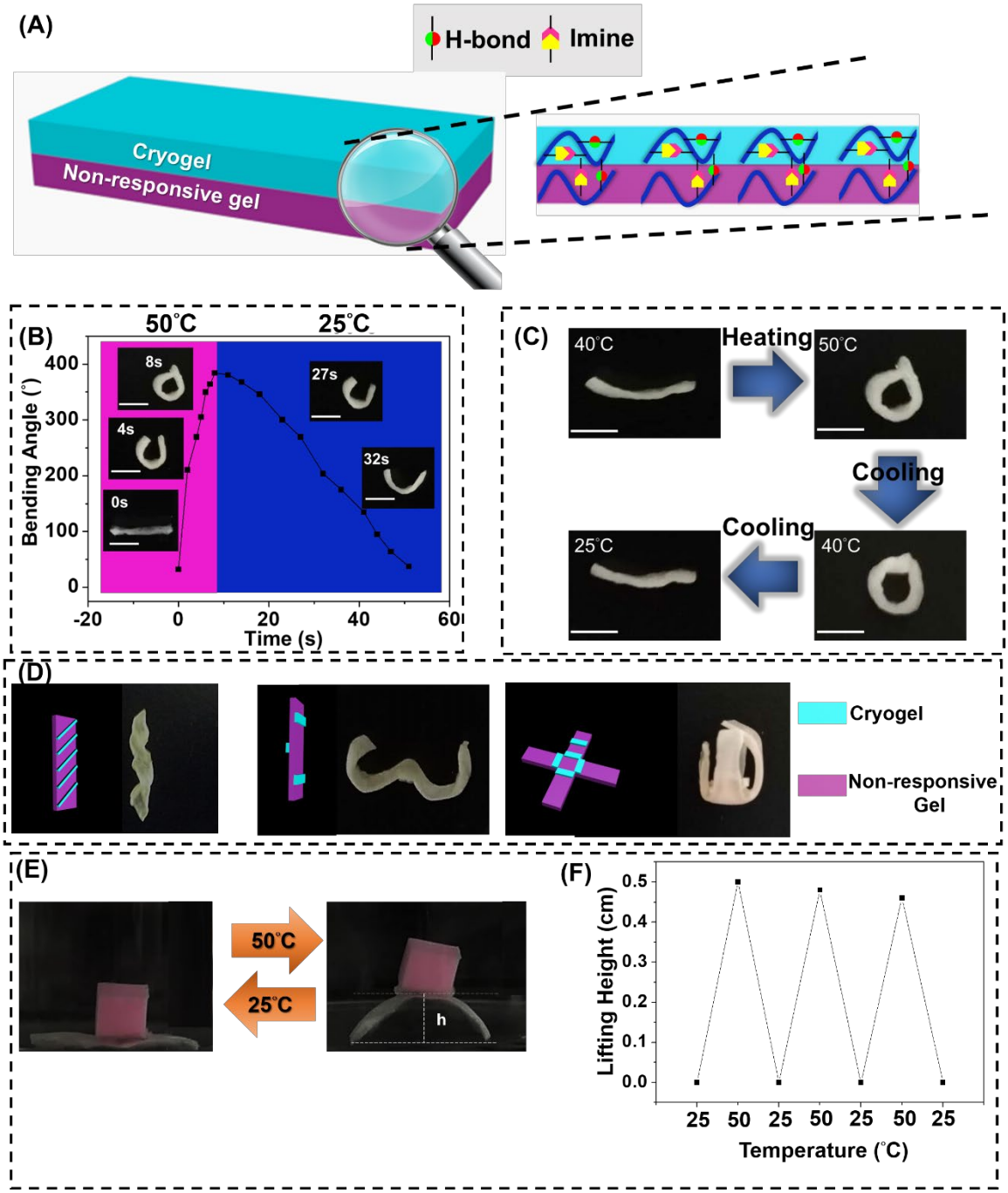

Figure 4. Shape changing properties of bilayer gels assembled from a freeze-thawed film with a non-responsive gel. (A) Schematic illustration of the preparation of double layer structure and dynamic interaction between the interface. (B) Variation of bending angles of the bilayer gels with time after incubation in 50 °C hot water and then 25 °C pure water. Inset shows the photographs of the bending of freeze-thawed hydrogel. (C) Photographs of the folding and unfolding of the bilayer freeze-thawed hydrogel in a heating-cooling cycle, showing thermal hysteresis behaviour at 40 °C, which result in the memory function. (D)

Various complex 3D temporary shapes achieved through tailoring the geometry of bonded gel slabs. (E) Photographs of bilayer freeze-thawed hydrogel loaded with silicone of tenfold the weight of the dried-hydrogel in middle. (F) Variation of the lifting height after periodic switching of the water temperature.

Studies of the aqueous solution behaviour of linear poly(MAA$_{113}$-*co*-BA$_{37}$-OEGMA$_{50}$) suggest that, upon heating, a change in transmittance occurs at 46 °C (Figure S8). However, pronounced thermal hysteresis was observed upon cooling, with the LCST observed at 34°C. Such LCST differences during heating and cooling processes could be explained by the formation of stable aggregates during heating due to very strong hydrophobic and inter-chain hydrogen bonding.[32a] This large thermal hysteresis loop may cause the memory functionality of our hydrogel system.[55] In order to test our hypothesis, the bilayer gel was firstly immersed into water at 40°C. No obvious bending was observed due to the highly swollen state of the freeze-thawed hydrogel at this temperature below LCST (Figure 4C). Significant shape changing was then observed at 50°C which is above the LCST. Interestingly, when the temperature of water returned to 40°C, the actuated folding state was maintained, even after 24 hours, suggesting the freeze-thawed hydrogel had memory function (Figure 4C). Further cooling erased this memory effect and the bilayer gel unfolded into a flat state (Figure 4C). It is worth noting that such cooling induced shape recovery is distinct from other traditional shape memory polymers which require heating to return it to their permanent shape[5a] which may result in irreversible tissue damage in biomedical applications. Using a similar process, other complex 3D structures could temporarily be created by through tailoring the geometry of bonded gel slabs (Figure 4D). This offers an opportunity to achieve complex temporary shapes in a non-contact and highly precise way by taking advantage of excellent self-healing behaviour, illustrating improvement compared to traditional thermo-induced shape memory polymers.[5a, 25b] Moreover, due to the broadly tunable LCST of the OEGMA unit,[56] we have

demonstrated a triple-shape-memory effect by combining another freeze-thawed hydrogel with a different LCST (Experiment section, Figure S14).

Finally, we demonstrated that these shape changing freeze-thawed hydrogels could perform useful functions. One step toward this is the ability for the freeze-thawed hydrogels to perform physical work. Here we demonstrate that the freeze-thawed hydrogel could repeatably lift and lower a weight fiftyfold the weight of the dried hydrogel. The silicon weight was loaded in the middle of a bilayer slab and temperature oscillations below and above the LCST enabled repeated lifting of the object. The object was readily, and repeatedly, lifted up to 0.6 cm after 90s due to the bending deformation of the bilayer gel slabs (Figure 4E), this process could be repeated (Figure 4F). This result demonstrates the possibility of using such doubly dynamic hydrogels with multiple functions in potential artificial muscles and soft actuator applications.

Conclusion

In summary, we have developed an innovative but simple molecular design strategy to prepare a dynamic hydrogel with a number of superior material properties including strength, toughness, fatigue-resistance, self-healing, rapid shape changing, and memory effect. Importantly, our designs reveal a successful balance between these often opposing properties into advanced materials with a combination of excellent material properties. The material system is based on the combination of the highly dynamic acid-ether hydrogen bonding and imine bonds, which could interact in a synergistic way to impart these unprecedented properties. We envision that this molecular design strategy could be extended into other stimuli-responsive shape changing polymers. Moreover, this dynamic material system can be facilely prepared using simple chemistry. A variety of other functional polymers can also be prepared by taking advantage of the potential reaction sites of carboxylic and aldehyde

groups. These demonstrations clearly indicate that our doubly dynamic hydrogels are promising for improving the flexibility and versatility of hydrogel applications such as next-generation soft robotics, artificial muscles and biomedical devices.

Experimental Section

Materials: All chemicals were obtained from Sigma Aldrich and used as received unless otherwise specified. Deionized water was produced by an ELGA Laboratory water station and had a resistivity of 18.2 m/cm. To remove inhibitors, oligoethyleneglycol methyl ether methacrylate [500 g mol^{-1},OEGMA] and methacrylic acid were passed through a basic alumina column immediately before use. 2,2'-azobis(2-methylpropionitrile) (AIBN) was recrystallized from methanol twice. Membranes for dialysis (molecular weight cut-off of 3500 Da) were purchased from Thermo Fisher Scientific.

Synthesis of Poly(MAA-co-OEGMA)
The procedure for preparation of well-defined poly(MAA-*co*-OEGMA) copolymers via RAFT polymerization is illustrated in Scheme 1. As a representative example, OEGMA 500 (2.78 mL), MAA (1.19 mL), 2-cyano-2-propyl benzodithioate (CDTPA) (0.1 mmol, 28.25 mg), and AIBN (3.36 mg), were dissolved in anhydrous DMSO (4.0 mL). The flask was sealed with a rubber septum and the solution was deoxygenated by sparging with nitrogen for 10 min. After polymerizing for 24 h at 65 °C, the reaction was cooled to 0 °C in an ice batch and exposed to air. The viscous polymer solution was diluted with DMSO and precipitated into diethyl ether three times, and then further purified by extensive dialysis in water. Copolymer of MAA and OEGMA initial feed ratios 85/15 was prepared using the same procedure for fabricating nonresponsive layer.

Post-modification of Poly(MAA-co-OEGMA)
Poly(MAA-co-OEGMA) (581 mg), 4-hydroxybenzaldahyde (308.6 mg), 4-(dimethylamino)pyridine (DMAP) (31 mg) and DCC (522 mg) were separately dissolved in anhydrous DMF, which were then combined under stirring. The reaction lasted for 22h. After filtration, the liquid was collected and precipitated into methanol, and then further purified by extensive dialysis in mixtures of water/methanol. The functionalized copolymer was filtered, collected and dried under vacuum.

Preparation of dynamic imine crosslinker hydrogel
The gel was prepared from functionalized copolymer by crosslinking with EDA (molar ratio of 1: 0.25, aldehyde: EDA). Functionalized copolymer (350 mg) was dissolved in DMF (2 mL) until a fully transparent and homogeneous solution was obtained. A stock solution of the crosslinker was prepared by dissolving a calculated amount of EDA in DMF. An aliquot of the stock solution (0.1 mL) was introduced to the dissolved polymer at ambient temperature. After 20 min, the solution was coated on a PTFE mould followed by heating at 50°C overnight to dry the sample. Furthermore, the hydrogel was dialyzed against DI water (48 h) and ethanol (24 h), respectively. In the beaker DI water was changed 6–8 times and ethanol was replaced 4–6 times after 2–10 h. Finally, all gels were dried under high vacuum at 40 °C for two days. The hydrogel slab could be easily peeled off from the PTFE mould. The hydrogel slabs with different crosslinking densities were prepared using the same procedure.

Preparation of the freeze-thawed hydrogels

After equilibrating the EDA crosslinked hydrogels in water for 24 h, the samples were then transferred into a freezer with a temperature of −20 °C for 8 h, which was followed by thawing at room temperature for at least 5 h. The freeze-thawed hydrogel-1 was also prepared using the same method (feed ratio of MAA and OEGMA is 67:33) for achieving a triple memory effect (discussed in Figure S14)

Measurement of water uptake:

To measure the water uptake values by gravimetric analysis, a small piece of hydrogel was taken in a beaker and immersed in DI water at different temperatures for 24 h to attain the maximum swelling ratio. Three duplicate samples of each hydrogel were prepared for swelling experiments to guarantee the reproducibility. Then, the swollen hydrogels were taken out of the water and weighed after removing excess water on the surface. The ESR was calculated from the following equation.

$$\text{Water uptake (\%)} = (W_s - W_d)/W_d \times 100$$

where W_s and W_d are the weights of swollen hydrogel in equilibrium and the corresponding dried hydrogel, respectively.

Characterization

^{1}H NMR (500 MHz) spectra were recorded using a Bruker Avance BB 500. Chemical shifts were recorded in ppm (δ). ^{1}H diffusion-ordered spectra (^{1}H DOSY) spectra were acquired from solutions of the polymer in D_2O and $CDCl_3$ using a Bruker Avance 700 MHz. The average sizes of the aggregates of the polymers was calculated using the Stokes−Einstein equation.[57] Infrared spectra of various hydrogels were acquired using a Nicolet 5700 Fourier transform infrared (FTIR) spectrometer fitted with an attenuated total reflectance (ATR) accessory that used a diamond internal reflection element (IRE) and the angle of incidence of the beam was fixed at 45˚ relative to the IRE. Thirty-two scans were averaged over a range of 500 to 4000 cm^{-1} at a resolution of 4 cm^{-1}. UV−vis measurements were conducted on a Varian UV-vis Cary 4000 spectrophotometer fitted with a Cary temperature controller to determine the LCST of copolymers in water. The LCST were calculated as the temperatures at which the transmittance decreased by 50% (at 500 nm). The heating rate was 1 °C min^{-1}. Mechanical properties of the hydrogels were measured by tensile tests using a commercial tensile tester. The samples were cut from the hydrogel sheets into a rectangular shape with length of 12 mm, width of 2 mm and thickness of 0.17 mm. The stretching rate is 60 mm min^{-1}. The nominal stress-strain curves were recorded, and the Young's modulus was calculated from the initial slope of the curve with a strain below 8%. Dynamic mechanical analysis (DMA) was performed to the hydrogels using a DMA 8000 dynamic mechanical analyzer. A disk sample (diameter = 1 cm, thickness = 0.2 mm) was cut from the bulk hydrogel. The test was run in a shear mode with a frequency of 1 Hz when the temperature increased from 5 to 50 °C (heating rate: 1 °C min^{-1}). Confocal laser scanning microscopy (CLSM) was performed on a Zeiss LSM780 UV-NLO confocal microscope using a laser excitation wavelength of 561 nm. Shape changing properties of hydrogels were recorded using a digital camera in a cell phone.

Supporting Information

Supporting Information is available from the Wiley Online Library or from the author.

Acknowledgements

Funding is gratefully acknowledged from the Australian Research Council (DP180103918), and the ANU Futures Scheme. The authors thank Associate Professor Zbigniew Stachurski for assistance with tensile testing. The dynamic mechanical analysis was collected with the assistance of Prof. Takuya Tsuzuki and Dr. Mahdiar Taheri. The ^{1}H diffusion-ordered spectra (^{1}H DOSY) spectra was collected with the assistance of Dr. Chris Blake. The authors would

like to thank Mr Daryl Webb for his assistance with CLSM, and Miss Heather Aitken for proofreading language in this manuscript. The authors also acknowledge the facilities and the scientific and technical assistance of Microscopy Australia at the Advanced Imaging Precinct, Australian National University, a facility that is funded by the University, and State and Federal Governments.

Conflict of Interest

The authors declare no conflict of interest.

ToC text: A multi-functional shape changing hydrogel was fabricated through rational design of dynamic networks. By harnessing acid-ether hydrogen bonding and imine bonds, high strength/toughness, fast self-healing, rapid and programmable actuation, as well as memory effect were simultaneously achieved. This material design strategy offers an avenue for synergistically engineering the properties of hydrogel actuators that are promising in diverse applications.

Keyword: Responsive shape changing hydrogels, self-healing, multi-functional hydrogel, multiple dynamic bonds, high strength

Zhen Jiang, Broden Diggle, India C.G. Shackleford, Luke A. Connal*

Rational design of multiple dynamic bonds to create tough, self-healing hydrogels with ultra-fast shape changing and memory function

ToC figure ((Please choose one size: 55 mm broad × 50 mm high **or** 110 mm broad × 20 mm high. Please do not use any other dimensions))

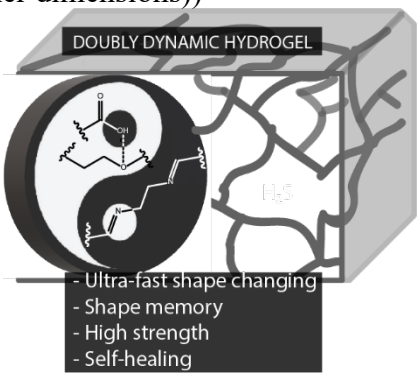

Reference

[1] Y. Forterre, J. M. Skotheim, J. Dumais, L. Mahadevan, *Nature* **2005**, 433, 421.

[2] C. Dawson, J. F. Vincent, A.-M. Rocca, *Nature* **1997**, 390, 668.

[3] B. Kim, D.-H. Kim, J. Jung, J.-O. Park, *Smart Mater. Struct.* **2005**, 14, 1579.

[4] J. R. Capadona, K. Shanmuganathan, D. J. Tyler, S. J. Rowan, C. Weder, *Science* **2008**, 319, 1370.

[5] a) C. Lowenberg, M. Balk, C. Wischke, M. Behl, A. Lendlein, *Acc. Chem. Res.* **2017**, 50, 723; b) W. Lu, X. Le, J. Zhang, Y. Huang, T. Chen, *Chem. Soc. Rev.* **2017**, 46, 1284; c) A. Lendlein, O. E. C. Gould, *Nat. Rev. Mater.* **2019**, 4, 116.

[6] a) Z. Pei, Y. Yang, Q. Chen, E. M. Terentjev, Y. Wei, Y. Ji, *Nat. Mater.* **2014**, 13, 36; b) Y. Yu, M. Nakano, T. Ikeda, *Nature* **2003**, 425, 145; c) J.-a. Lv, Y. Liu, J. Wei, E. Chen, L. Qin, Y. Yu, *Nature* **2016**, 537, 179; d) Z. Jiang, M. Xu, F. Li, Y. Yu, *J. Am. Chem. Soc.* **2013**, 135, 16446; e) F. Ge, R. Yang, X. Tong, F. Camerel, Y. Zhao, *Angew. Chem. Int. Ed.* **2018**, 57, 11758.

[7] a) A. Nojoomi, H. Arslan, K. Lee, K. Yum, *Nat. Commun.* **2018**, 9, 3705; b) X. Du, H. Cui, Q. Zhao, J. Wang, H. Chen, Y. Wang, *Research* **2019**, 2019, 1; c) S. J. Jeon, A. W. Hauser, R. C. Hayward, *Acc. Chem. Res.* **2017**, 50, 161; d) O. Erol, A. Pantula, W. Liu, D. H. Gracias, *Adv. Mater. Tech.* **2019**, DOI: 10.1002/admt.2019000431900043; e) L. Ionov, *Adv. Func. Mater.* **2013**, 23, 4555; f) X. Le, W. Lu, J. Zhang, T. Chen, *Adv. Sci.* **2019**, DOI: 10.1002/advs.2018015841801584.

[8] a) B. Han, Y. L. Zhang, Q. D. Chen, H. B. Sun, *Adv. Func. Mater.* **2018**, 28, 1802235; b) W. Xu, K. S. Kwok, D. H. Gracias, *Acc. Chem. Res.* **2018**, 51, 436.

[9] Y. Liu, J. Genzer, M. D. Dickey, *Prog. Polym. Sci.* **2016**, 52, 79.

[10] G. M. Whitesides, *Angew. Chem. Int. Ed.* **2018**, 57, 4258.

[11] J. ter Schiphorst, S. Coleman, J. E. Stumpel, A. Ben Azouz, D. Diamond, A. P. Schenning, *Chem. Mater.* **2015**, 27, 5925.

[12] V. Stroganov, J. Pant, G. Stoychev, A. Janke, D. Jehnichen, A. Fery, H. Handa, L. Ionov, *Adv. Func. Mater.* **2018**, 28, 1706248.

[13] S. Fusco, H.-W. Huang, K. E. Peyer, C. Peters, M. Häberli, A. Ulbers, A. Spyrogianni, E. Pellicer, J. Sort, S. E. Pratsinis, *ACS Appl. Mater. Interfaces* **2015**, 7, 6803.

[14] A. Kirillova, L. Ionov, *J. Mater. Chem. B* **2019**, DOI: 10.1039/c8tb02579g.

[15] a) L. Huang, R. Jiang, J. Wu, J. Song, H. Bai, B. Li, Q. Zhao, T. Xie, *Adv. Mater.* **2017**, 29; b) C. Ma, T. Li, Q. Zhao, X. Yang, J. Wu, Y. Luo, T. Xie, *Adv. Mater.* **2014**, 26, 5665; c) Z. Sun, Y. Yamauchi, F. Araoka, Y. S. Kim, J. Bergueiro, Y. Ishida, Y. Ebina, T. Sasaki, T. Hikima, T. Aida, *Angew. Chem. Int. Ed.* **2018**, 57, 15772; d) A. S. Gladman, E. A. Matsumoto, R. G. Nuzzo, L. Mahadevan, J. A. Lewis, *Nat. Mater.* **2016**, 15, 413; e) Z. L. Wu, M. Moshe, J. Greener, H. Therien-Aubin, Z. Nie, E. Sharon, E. Kumacheva, *Nat. Commun.* **2013**, 4, 1586; f) C. Ma, X. Le, X. Tang, J. He, P. Xiao, J. Zheng, H. Xiao, W. Lu, J. Zhang, Y. Huang, T. Chen, *Adv. Func. Mater.* **2016**, 26, 8670.

[16] a) T. Chen, H. Bakhshi, L. Liu, J. Ji, S. Agarwal, *Adv. Func. Mater.* **2018**, 28, 1800514; b) W. Fan, C. Shan, H. Guo, J. Sang, R. Wang, R. Zheng, K. Sui, Z. Nie, *Sci. Adv.* **2019**, 5, eaav7174; c) J. Wang, J. Wang, Z. Chen, S. Fang, Y. Zhu, R. H. Baughman, L. Jiang, *Chem. Mater.* **2017**, 29, 9793.

[17] a) S. Y. Zheng, Y. Shen, F. Zhu, J. Yin, J. Qian, J. Fu, Z. L. Wu, Q. Zheng, *Adv. Func. Mater.* **2018**, 28, 1803366; b) L. W. Xia, R. Xie, X. J. Ju, W. Wang, Q. Chen, L. Y. Chu, *Nat. Commun.* **2013**, 4, 2226; c) H. Cui, N. Pan, W. Fan, C. Liu, Y. Li, Y. Xia, K. Sui, *Adv. Func. Mater.* **2019**, 1807692; d) P. Sun, H. Zhang, D. Xu, Z. Wang, L. Wang, G. Gao, G. Hossain, J. Wu, R. Wang, J. Fu, *J. Mater. Chem. B* **2019**, DOI: 10.1039/c9tb00249a.

[18] a) J. Shang, X. Le, J. Zhang, T. Chen, P. Theato, *Poly. Chem.* **2019**, DOI: 10.1039/c8py01286e; b) F. Zhang, L. Xiong, Y. Ai, Z. Liang, Q. Liang, *Adv. Sci.* **2018**, 5, 1800450; c) F. X. Wang, Q. Li, S. S. Liu, X. Y. Du, C. F. Wang, S. Chen, *Soft Matter* **2019**, 15, 2517; d) H. Qin, T. Zhang, N. Li, H.-P. Cong, S.-H. Yu, *Nat. Commun.* **2019**, 10.
[19] L. Wang, Y. Jian, X. Le, W. Lu, C. Ma, J. Zhang, Y. Huang, C. F. Huang, T. Chen, *Chem. Commun.* **2018**, 54, 1229.
[20] C. Ma, W. Lu, X. Yang, J. He, X. Le, L. Wang, J. Zhang, M. J. Serpe, Y. Huang, T. Chen, *Adv. Func. Mater.* **2018**, 28, 1704568.
[21] a) P. Chakma, D. Konkolewicz, *Angew. Chem. Int. Ed.* **2019**, DOI: 10.1002/anie.201813525; b) W. Zou, J. Dong, Y. Luo, Q. Zhao, T. Xie, *Adv. Mater.* **2017**, 29; c) Z. P. Zhang, M. Z. Rong, M. Q. Zhang, *Prog. Polym. Sci.* **2018**, 80, 39; d) Z. Jiang, A. Bhaskaran, H. M. Aitken, I. C. Shackleford, L. A. Connal, *Macromol. Rapid. Commun.* **2019**, 1900038.
[22] a) T. L. Sun, T. Kurokawa, S. Kuroda, A. B. Ihsan, T. Akasaki, K. Sato, M. A. Haque, T. Nakajima, J. P. Gong, *Nat. Mater.* **2013**, 12, 932; b) W. Wang, Y. Zhang, W. Liu, *Prog. Polym. Sci.* **2017**, 71, 1; c) Y. Yang, X. Wang, F. Yang, L. Wang, D. Wu, *Adv. Mater.* **2018**, 30, e1707071; d) L. Zhang, Z. Liu, X. Wu, Q. Guan, S. Chen, L. Sun, Y. Guo, S. Wang, J. Song, E. M. Jeffries, C. He, F. L. Qing, X. Bao, Z. You, *Adv. Mater.* **2019**, DOI: 10.1002/adma.201901402e1901402; e) Y. Song, Y. Liu, T. Qi, G. L. Li, *Angew. Chem. Int. Ed.* **2018**, 57, 13838.
[23] L. Chen, R. Liu, X. Hao, Q. Yan, *Angew. Chem. Int. Ed.* **2019**, 58, 264.
[24] a) D. L. Taylor, M. In Het Panhuis, *Adv. Mater.* **2016**, 28, 9060; b) M. Guo, L. M. Pitet, H. M. Wyss, M. Vos, P. Y. Dankers, E. Meijer, *J. Am. Chem. Soc.* **2014**, 136, 6969.
[25] a) X. Hu, D. Zhang, S. S. Sheiko, *Adv. Mater.* **2018**, 30, e1707461; b) Q. Zhao, H. J. Qi, T. Xie, *Prog. Polym. Sci.* **2015**, 49-50, 79.
[26] a) L. Li, Q. Lin, M. Tang, A. J. E. Duncan, C. Ke, *Chem. Asian. J.* **2019**, DOI: 10.1002/chem.201900975; b) T. Jungst, W. Smolan, K. Schacht, T. Scheibel, J. Groll, *Chem. Rev.* **2016**, 116, 1496; c) X. F. Zhang, X. Ma, T. Hou, K. Guo, J. Yin, Z. Wang, L. Shu, M. He, J. Yao, *Angew. Chem. Int. Ed.* **2019**, DOI: 10.1002/anie.201902578.
[27] R. J. Wojtecki, M. A. Meador, S. J. Rowan, *Nat. Mater.* **2011**, 10, 14.
[28] L. Tang, L. Wen, S. Xu, P. Pi, X. Wen, *Chem. Commun.* **2018**, 54, 8084.
[29] Q. Zhang, C.-Y. Shi, D.-H. Qu, Y.-T. Long, B. L. Feringa, H. Tian, *Sci. Adv.* **2018**, 4, eaat8192.
[30] P. Wang, G. Deng, L. Zhou, Z. Li, Y. Chen, *ACS Macro Lett.* **2017**, 6, 881.
[31] E. R. Draper, E. G. Eden, T. O. McDonald, D. J. Adams, *Nat. Chem.* **2015**, 7, 848.
[32] a) J. A. Jones, N. Novo, K. Flagler, C. D. Pagnucco, S. Carew, C. Cheong, X. Z. Kong, N. A. Burke, H. D. Stöver, *J. Polym. Sci. A* **2005**, 43, 6095; b) S. Naficy, J. M. Razal, P. G. Whitten, G. G. Wallace, G. M. Spinks, *J. Polym. Sci. A* **2012**, 50, 423.
[33] W.-C. Liu, C.-H. Chung, J.-L. Hong, *ACS Omega* **2018**, 3, 11368.
[34] a) Z. Jiang, I. Blakey, A. K. Whittaker, *Poly. Chem.* **2017**, 8, 4114; b) Z. Jiang, H.-H. Cheng, I. Blakey, A. K. Whittaker, *Mol. Syst. Des. Eng.* **2018**, 3, 627.
[35] Z. Jiang, R. J. P. Sanchez, I. Blakey, A. K. Whittaker, *Chem. Commun.* **2018**, 54, 10909.
[36] C. Zhang, H. Peng, A. K. Whittaker, *J. Polym. Sci. A* **2014**, 52, 2375.
[37] Y. Cao, Y. Guan, J. Du, J. Luo, Y. Peng, C. Yip, A. S. Chan, *J. Mater. Chem.* **2002**, 12, 2957.
[38] D. Rinaldi, T. Hamaide, C. Graillat, F. D'Agosto, R. Spitz, S. Georges, M. Mosquet, P. Maitrasse, *J. Polym. Sci. A* **2009**, 47, 3045.

[39] a) M. Nadgorny, Z. Xiao, L. A. Connal, *Mol. Syst. Des. Eng.* **2017**, 2, 283; b) S. Bhattacharya, R. S. Phatake, S. Nabha Barnea, N. Zerby, J. J. Zhu, R. Shikler, N. G. Lemcoff, R. Jelinek, *ACS Nano* **2019**, DOI: 10.1021/acsnano.8b07087; c) M. Kathan, P. Kovaříček, C. Jurissek, A. Senf, A. Dallmann, A. F. Thünemann, S. Hecht, *Angew. Chem. Int. Ed.* **2016**, 55, 13882.

[40] a) D. Chen, Y. Zhang, C. Ni, C. Ma, J. Yin, H. Bai, Y. Luo, F. Huang, T. Xie, Q. Zhao, *Mater. Horiz.* **2019**, DOI: 10.1039/c9mh00090a; b) M. Nadgorny, J. Collins, Z. Xiao, P. J. Scales, L. A. Connal, *Poly. Chem.* **2018**, 9, 1684; c) K. Iwaso, Y. Takashima, A. Harada, *Nat. Chem.* **2016**, 8, 625.

[41] a) Y. J. Wang, X. N. Zhang, Y. Song, Y. Zhao, L. Chen, F. Su, L. Li, Z. L. Wu, Q. Zheng, *Chem. Mater.* **2019**, DOI: 10.1021/acs.chemmater.8b05262; b) H. Fan, J. Wang, Z. Jin, *Macromolecules* **2018**, 51, 1696; c) T. Liu, C. Jiao, X. Peng, Y.-N. Chen, Y. Chen, C. He, R. Liu, H. Wang, *J. Mater. Chem. B* **2018**, DOI: 10.1039/c8tb02556h.

[42] H. Guo, J. Cheng, J. Wang, P. Huang, Y. Liu, Z. Jia, X. Chen, K. Sui, T. Li, Z. Nie, *J. Mater. Chem. B* **2017**, 5, 2883.

[43] K. Jin, A. Banerji, D. Kitto, F. S. Bates, C. J. Ellison, *ACS Appl. Mater. Interfaces* **2019**, 11, 12863.

[44] J. Y. Sun, X. Zhao, W. R. Illeperuma, O. Chaudhuri, K. H. Oh, D. J. Mooney, J. J. Vlassak, Z. Suo, *Nature* **2012**, 489, 133.

[45] J. P. Gong, *Soft Matter* **2010**, 6, 2583.

[46] X. Yan, Z. Liu, Q. Zhang, J. Lopez, H. Wang, H. C. Wu, S. Niu, H. Yan, S. Wang, T. Lei, J. Li, D. Qi, P. Huang, J. Huang, Y. Zhang, Y. Wang, G. Li, J. B. Tok, X. Chen, Z. Bao, *J. Am. Chem. Soc.* **2018**, 140, 5280.

[47] a) S. Xiao, M. Zhang, X. He, L. Huang, Y. Zhang, B. Ren, M. Zhong, Y. Chang, J. Yang, J. Zheng, *ACS Appl. Mater. Interfaces* **2018**, 10, 21642; b) Y. Zhang, J. Liao, T. Wang, W. Sun, Z. Tong, *Adv. Func. Mater.* **2018**, 28, 1707245; c) S. E. Bakarich, R. Gorkin, 3rd, M. in het Panhuis, G. M. Spinks, *Macromol. Rapid. Commun.* **2015**, 36, 1211; d) Y. Tan, D. Wang, H. Xu, Y. Yang, W. An, L. Yu, Z. Xiao, S. Xu, *Macromol. Rapid. Commun.* **2018**, 39, e1700863; e) J. M. Boothby, J. Samuel, T. H. Ware, *Soft Matter* **2019**, DOI: 10.1039/c9sm00763f.

[48] J. Fu, *J. Polym. Sci. B* **2018**, 56, 1279.

[49] J. A. Neal, D. Mozhdehi, Z. Guan, *J. Am. Chem. Soc.* **2015**, 137, 4846.

[50] J. Kang, D. Son, G. J. N. Wang, Y. Liu, J. Lopez, Y. Kim, J. Y. Oh, T. Katsumata, J. Mun, Y. Lee, *Adv. Mater.* **2018**, 30, 1706846.

[51] D.-P. Wang, Z.-H. Zhao, C.-H. Li, J.-L. Zuo, *Mater. Chem. Front.* **2019**, DOI: 10.1039/c9qm00115h.

[52] a) Y. Lai, X. Kuang, P. Zhu, M. Huang, X. Dong, D. Wang, *Adv. Mater.* **2018**, 30, 1802556; b) H. Zhang, H. Xia, Y. Zhao, *ACS Macro Lett.* **2012**, 1, 1233.

[53] T. van Manen, S. Janbaz, A. A. Zadpoor, *Mater. Today* **2018**, 21, 144.

[54] a) H. Therien-Aubin, Z. L. Wu, Z. Nie, E. Kumacheva, *J. Am. Chem. Soc.* **2013**, 135, 4834; b) E. Wang, M. S. Desai, S. W. Lee, *Nano. Lett.* **2013**, 13, 2826; c) S. Y. Zheng, Y. Tian, X. N. Zhang, M. Du, Y. Song, Z. L. Wu, Q. Zheng, *Soft Matter* **2018**, 14, 5888; d) W. J. Zheng, N. An, J. H. Yang, J. Zhou, Y. M. Chen, *ACS Appl Mater Interfaces* **2015**, 7, 1758; e) Y. Tan, D. Wang, H. Xu, Y. Yang, X. L. Wang, F. Tian, P. Xu, W. An, X. Zhao, S. Xu, *ACS Appl. Mater. Interfaces* **2018**, 10, 40125; f) J. Tang, Z. Tong, Y. Xia, M. Liu, Z. Lv, Y. Gao, T. Lu, S. Xie, Y. Pei, D. Fang, T. J. Wang, *J. Mater. Chem. B* **2018**, 6, 2713.

[55] a) D. Kim, H. Kim, E. Lee, K. S. Jin, J. Yoon, *Chem. Mater.* **2016**, 28, 8807; b) K. Zhang, X. Feng, C. Ye, M. A. Hempenius, G. J. Vancso, *J. Am. Chem. Soc.* **2017**, 139, 10029; c) X. Hu, D. Zhang, S. S. Sheiko, *Adv. Mater.* **2018**, 30, 1707461.

[56] C. Zhang, H. Peng, S. Puttick, J. Reid, S. Bernardi, D. J. Searles, A. K. Whittaker, *Macromolecules* **2015**, 48, 3310.
[57] C. Zhang, H. Peng, W. Li, L. Liu, S. Puttick, J. Reid, S. Bernardi, D. J. Searles, A. Zhang, A. K. Whittaker, *Macromolecules* **2016**, 49, 900.